Proceedings of the International Symposium on Room Acoustics, ISRA 2010

29-31 August 2010, Melbourne, Australia

A combination of the sound particle simulation method and the radiosity method

Alexander Pohl and Uwe M. Stephenson

HafenCity University, Hamburg, Germany

PACS: 43.55.KA, 43.58.TA, 43.20.EL, 43.20.DK, 43.20.FN

ABSTRACT

In room and urban acoustics, ray tracing as well as, for the reverberation tail, radiosity based simulation methods are in use. Any implementation of diffraction into the sound particle simulation method, i.e. a variant of ray tracing, causes a split-up of sound particles and an explosion of computation time. To prevent that, a re-unification effect of sound energies has to be achieved as known from the radiosity method. For this purpose, the discretization of the walls into small patches is applied to the sound particle simulation method. This combination is called the sound particle radiosity method. In the main part of this paper the efficiency of the presented sound particle radiosity in investigated by deriving a statistical re-unification formula as a function of the main quantization parameter: the patch size. Furthermore the error due to quantization is described as a function of the patch size. It is shown, that smaller patches increase accuracy, but larger patches increase the efficiency. The smearing of echograms due to the receiver size mainly masks the quantization error when the receiver size is at least 10 times the patch size. This investigation, restricted to 2D, serves as a feasibility test for quantized pyramidal beam tracing.

INTRODUCTION

In room acoustics as well as in urban acoustics sound propagation has to be simulated efficiently. Wave-based simulation methods as the finite element method [1] or the boundary element method [2] include diffraction and scattering as a wave phenomena. But they cannot be used for large-scale models or high frequencies (as a thumb rule the size of the finite elements must not exceed about a sixth of the wavelength). On the other hand, the lack of geometric acoustic simulation methods such as the image source method [3], ray tracing [4], beam tracing [5] or the radiosity method [6], is, as a matter of principle, the missing diffraction.

Additional diffraction modules have to be introduced into geometric simulation methods. Only completely diffuse reflections according Lambert`s law [7] may be traced by ray tracing and are even exclusively possible with the radiosity method.

For the image source method, as an improvement to the well known detour law for diffraction, Svensson presented a secondary source model [8]. It computes diffraction coherently by integration over all secondary sources placed on the diffracting edge. Stephenson presented an energetic diffraction module based on the uncertainty principle that is applicable to beam as well as to ray tracing, interpreting beams and rays as carriers of sound energy [9]. In this approach, sound energy carriers are diffracted around edges corresponding to a diffraction angle probability density function depending on a by-pass distance.

To introduce diffraction as well as scattering into ray or beam tracing, a split-up of them is necessary to realize a suitable resolution in space. This split-up causes an exponential growth of the computation time for ray as well as for beam tracing, which prevents an efficient simulation of sound propagation.

To reduce this exponential growth of computation time, it is aimed at a re-unification of sound energy carriers. This is inspired by the radiosity method - where sound energy carriers are re-unified at each patch automatically. That re-unification is also the basis of quantized pyramidal beam tracing [10]. While quantized pyramidal beam tracing is not implemented and thus not evaluated, this paper aims, as a first approach, at a re-unification of rays instead of beams [10].

In this paper the idea of combining ray tracing with the radiosity method to a very efficient geometric simulation method including diffraction and scattering is described. To fade out the complex geometric algorithms and discuss the statistical effects, the study is limited to 2D.

Organization of the paper

In the first part of the paper the sound particle simulation method is described and the used diffraction and scattering models are presented. In the second part the re-unification of sound particles based on the radiosity method, first presented as the sound particle radiosity method by Stephenson [10], is repeated. In the main part of the paper, first time an implementation of the sound particle radiosity method is introduced. Besides the statistical evaluation of the efficiency of the method, the analytical error in simulation due to quantization is presented relative to the unquantized sound particle simulation method. Finally a recommended patch size as a trade-off between accuracy and efficiency is discussed in the conclusion.

THE SOUND PARTICLE SIMULATION METHOD

Ray tracing is one of the basic geometric acoustic simulation methods for sound propagation, especially for the simulation of reflections of higher orders. The idea is to emit a number of N sound energy carriers and trace them through the scene. Each sound energy carrier hitting a wall is reflected at the wall (geometrically or diffusely). With each reflection, called *iteration* later, the energy of the sound energy carrier is reduced by absorption [7].

The basic algorithm of the ray tracing can be described within three loops: over all sources, over all sound energy carriers, over all reflections. The process is shown in a flow chart in Figure 1.

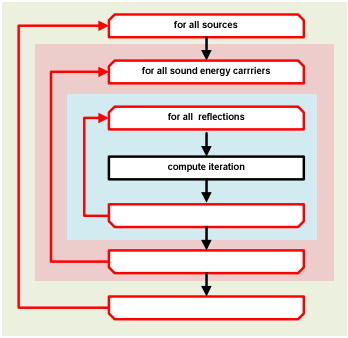

Figure 1. Flow chart of ray tracing. All sound energy carriers are traced within three loops. The outer loop is a loop over all sources; the middle loop is a loop over all sound energy carriers (per source). Finally the inner loop handles all reflections of a sound energy carrier, called *iteration*.

To detect the sound energy carriers, receivers have to be placed on the position, where the sound energy distribution is of interest. If a whole spatial sound distribution is wanted, a grid of receivers is chosen. Rays are infinitely thin lines. So the receivers have to be spatially extended to allow an intersection of sound energy carriers and receivers. This is the main difference to beam tracing, where the sound energy carriers are spatially extended beams and the receivers remain point-shaped. When a sound energy carrier, ray or beam, intersects with a receiver, its energy and delay time since emission from the source is counted in the receivers. The result is an energy-over-time distribution for each receiver, the echogram (see Figure 2).

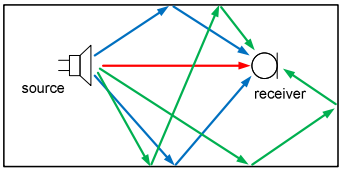

a) Geometric scene with sound paths

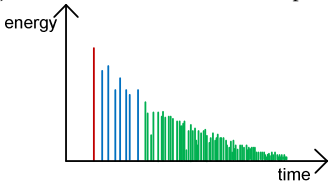

b) Echogram for specified source-receiver combination

Figure 2. Sound propagation in a simple rectangular, two-dimensional room. Sound can propagate from the source to the receiver in direct line (red, direct sound), over some reflections (blue, early reflections) or over many reflections (green, reverberation tail).

This echogram can be separated in three parts:

- direct sound
- early reflections
- reverberation tail

The direct sound describes the direct path between source and receiver and is most important for the source localisation. The early reflections describe sound paths from source to receiver over only a few walls. They are very important for speech intelligibility and source localization. The reverberation tail describes the reflections over many walls and allows conclusions of the room shape and size.

With ray tracing, spherical detectors detect, whether a ray intersects. Then the intensity of the respective mirror image source is computed according the $\frac{1}{r^2}$-law. With the sound particle simulation method (SPSM), the energy of crossing sound particles is also weighted with the time (or distance) the sound particles travel in the receivers [11].

As the SPSM is much simpler than BT [11] (only thin lines rather than a whole beam range) it is chosen here.

Convex sub-division

Speed-up techniques for ray tracing are based on spatial subdivision, because the most time consuming part of the simulation is the search for the next intersection point. One of these techniques reduces the needed time by dividing the scene into convex sub-scenes [12]. A second great benefit of convex sub-division is the detection of diffraction. While in a convex sub-scene no diffraction can occur, each intersection with a transparent wall, i.e. an inserted wall to separate sub-scenes, can be interpreted as a possible diffraction.

Scattering in the SPSM

The SPSM supports geometric or diffuse reflections (scattering on rough surfaces). Therefore, for each wall a scattering coefficient δ can be defined, which describes the ratio of scattered sound energy relative to the overall reflected energy. This scattered energy is independent of the incident angle.

There are different methods to implement the scattered energy. One is to draw a random number z between 0 and 1 and by that decide whether the ray is reflected diffusely or geometrically (if $z < \delta$ diffusely, else geometrically). If diffuse, another random number (in 3D: two) determines the direction in the half space.

A second possibility is to calculate the geometrically reflected direction as well as the random direction of a diffuse ray and add both direction vectors weighting the diffuse direction with δ and the geometric direction with $(1-\delta)$ (and then normalize to 1). Both methods have a low spatial resolution in common, because still only one sound particle is traced further on carrying the whole scattered energy. On the other hand there is no explosion of computation time due to no split-up of sound particles.

In our approach we keep the geometrically reflected energy of one sound particle and add a number S of *additional* scattered sound particles. These are equally distributed over the half space. (If only the portion f of the room's surface is scattering with a split-up of s, then the effective additional number of scattered sound particles is $S = f \cdot s$)

Diffraction in the SPSM

Some basic features of Stephenson`s method in short: Inspired by the uncertainty relation (interpreting the by-pass-distance as an 'uncertainty') the diffraction probability should be the stronger the closer the by-pass-distance a [9]. The diffraction angle probability density function (in short: D) is derived from the spatial Fourier transform of the transfer function of a slit, smoothed over a wide frequency band and simplified:

$$D(\varepsilon) = \frac{D_0}{1+2\cdot v^2} \quad \text{with} \quad v = 2 \cdot b_{eff} \cdot \varepsilon \qquad (1)$$

where b_{eff} is the apparent slit width measured in wavelengths λ, ε is the deflection angle and D_0 is a normalization factor (see Figure 3). From a self-consistency consideration follows that $b_{eff} = {}^1/_{6a}$

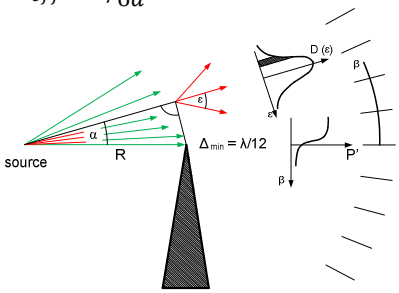

Figure 3. The sound particle diffraction model: Each moment a sound particle passes an edge at a distance a, it 'sees' a slit. According to the uncertainty relation certain edge diffraction strength causes the particle to be diffracted according to the diffraction angle probability density function = $D(\varepsilon)$. All the shifted diffraction angle probability density functions of the different sound particles add up to the screen transmission function.

The implementation is equal to the implementation of scattering. Again a number of S new sound particles is generated and equally distributed around the incident angle. Their energy is weighted regarding eqn. 1 and D_0 is defined such that the energy from $-\frac{\pi}{2} < \varepsilon < \frac{\pi}{2}$ is in sum 1.

RE-UNIFICATION OF SOUND PARTICLES

Exponential growth of the number of sound particles with split-up of sound particles due to reflection or scattering

To explain the growth of the number of sound particles due to split-up, we first abstract from the complete SPSM to the growth of a tree-structure (see Figure 5). The ordinate y of the tree is interpreted as the reflection order (including scattering and diffraction events) and the abscissa x of the tree-structure as the rolled up circumference of the scene. While in reality, after every reflection, the sound particle is on the circumference of the scene, it is in the tree symbolically on a node (x, y), representing its location x on the circumference after y reflections. Without split-up (typically with only geometric reflections) the number of sound particles remains constant to the number of emitted sound particles N. With split-up of sound particles due to diffraction (at transparent walls between convex sub-scenes) or scattering, the number of tree nodes (i.e. the number of sound particles) growths exponentially. The growth of such a tree-structure is shown in Figure 4a without and Figure 4b with split-up of sound particles.

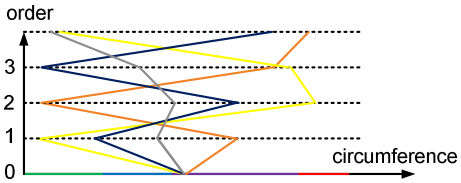

a) Structure of the tracing of four sound particles without split-up

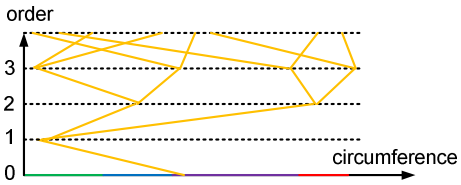

b) Structure of the tracing of one sound particle with split-up into two with each iteration (one additional sound particle i.e. $S = 1$)

Figure 4. Distribution of sound particles particles traced over the first four reflections symbolically in a tree structure. The x - coordinate of every node represents the particle's position on the circumference of the room, its y - value the reflection order.

Idea of re-unification: Quantization of space and directions

In the tree-structure with split-up (as in Figure 5b), the number of sound particles propagating in the same environment increases and thus the sound particles fill the environment with higher density. The interesting question is, if there are sound particles in such high density, which are equal or at least similar.

To reduce the computation effort, the idea is to search for those similar sound particles to re-unify. This would be completely inefficient if the search for similarly running sound particles would be *the whole time* (The time for searching would exceed time for tracing the sound particles by far). Hence, Stephenson presented an approach [10], where re-unification should only be allowed when sound particles intersect with the circumference (as sound particles do not change their direction between walls). Instead of the tedious searching for any similar sound particle, the sound particles are sorted into pre-defined memory spaces associated to small patches on the room's surface. This is the idea of quantization to allow re-unification adopted from the radiosity method.

Radiosity method

The radiosity method (also called radiance transfer method) is not a straight forward simulation like ray tracing, but calculates an energy exchange between all parts of the surface.

For the numerical implementation of the radiosity method, in a pre-processing phase, the whole surface is sub-divided into small patches and only once shape factors are computed describing energy transfer from any patch i to each other j (see Figure 5) [6].

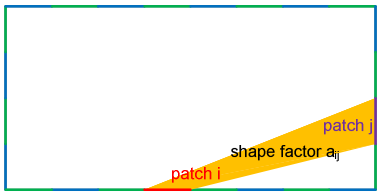

Figure 5. Separation of scene into small wall segments called patches. Shape factors for each patch-pair are calculated in a pre-processing step to describe the energy exchange between them.

To compute the stationary distribution the method ends up with a large linear equation system to be solved. As inherent to its functional principle, only diffuse reflections can be calculated ("forgetting the past of the sound particle").

The interesting and inspiring point of this method in our context is the re-unification of sound energy on each patch. The time dependent simulation consists of the organisation of a quasi-simultaneous energy exchange between patches.

Sound particle logistics

Even with a limitation of sound particle re-unification at wall intersections, still a very complicated part is the logistics of sound particles. In current sound particle simulation implementations, the sound particles are traced one after another (see Figure 1), but that inhibits a re-unification. For re-unification of sound particles, several sound particles must, of course, exist simultaneously, as shown in Figure 6.

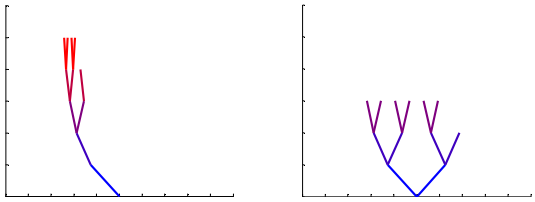

Figure 6. Comparison of sound particle propagation "one after another" (left) and quasi-parallel propagation (right) to allow re-unification

The algorithm of the SPSM has to be changed to an energy redistribution technique. All energies have to be stored after each reflection, a re-unification has to be made, and (in most cases) a different sound particle has to be traced further. After that there are only transient energy carriers left (the sound particles lose their 'individuality').

Intersection points are steadily distributed over the circumference (an infinite number of intersection points is possible). So a discretization of the positions and directions of a sound particle is necessary to recognize sound particles 'similar' to re-unify them. A similarity of sound particles to be re-unified is given if sound particles have:

- a similar intersection point with the room surface (i.e. practically hit the same patch),
- travel into a similar direction and
- hit the intersected wall about at the same time or travelled total distance from source.

Therefore, a quantization has to be performed with respect to these three variables.

The energy itself is not quantized. The energies of formerly different incident particles are traced in a combined sound particle that carries the sum of all input particle energies.

The idea of the quantization of positions on the surface is overtaken from the radiosity method; the idea of quantization of directions is retained from the SPSM.

Hence, the whole method changes to a universal energy redistribution method allowing as well geometric or diffuse reflections as diffractions of arbitrary order without explosion of computation time. Thus, the combined "Sound Particle Radiosity Method" (SPRADM) is able to handle geometric as well as diffuse reflections or scatterings and diffractions in a unified way without explosion of computation time. The discretization of sound particles as well as the complex logistics are part of the realisation of SPRADM.

THE SOUND PARTICLE RADIOSITY METHOD

The Algorithm of the SPRADM

To realize the spatial quantization, in a pre-processing phase the whole circumference (in 3D: surface) of the 'room' is split up into patches of a specified length l_P.

The flow chart of SPRADM can be separated in two parts. First the matrix has to be initialised with energies from the original source to be traced. In the further steps these energies, i.e. the energy carriers, have to be traced through the scene. Both parts are shown in a flow chart in Figure 7.

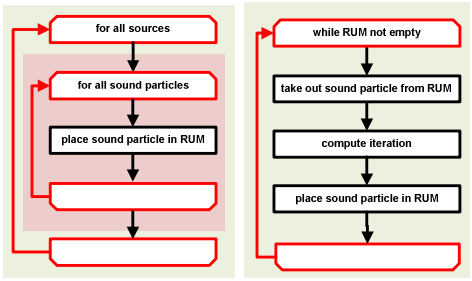

Figure 7. Flow chart of SPRADM. In an initialisation step (left) all sound particles for all sources (former two outer loops of SPSM, see Figure 1) have to be placed in the re-unification matrix (RUM). The simulation itself works off the RUM. Sound particles are taken out of the RUM, traced for one iteration, and are added back to the RUM.

Introduction of a quantization and re-unification matrix (RUM)

For the implementation of the sound particle radiosity method (SPRADM), the usage of a re-unification matrix (RUM) is introduced.

To realize the directional quantization, a special realisation technique is to substitute the sound particle direction by its end point, i.e. its target patch. To make the number of patches independent from the room size, it may be related to the mean free path length (MFPL) $\bar{l}$. A quantization factor f_P (< 1) is then

$$f_P = \frac{l_P}{\bar{l}} \tag{2a}$$

Another quantization factor g_P (preferred below, $g_P > 1$) is the number of patches the circumference C is sub-divided in:

$$g_P = \frac{C}{l_P} = \frac{C}{\bar{l}} \cdot \frac{1}{f_P} \tag{2b}$$

During run-time of the simulation, every intersection point of a sound particle with the wall is moved to the middle of the patch (see Figure 8).

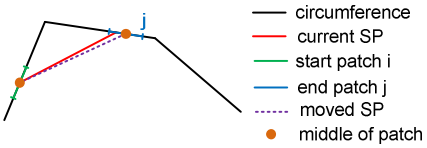

Figure 8. Alteration of a current sound particle's path by quantization of the end patch: the calculated hit point is moved to the middle of a patch. Automatically the start point of the next iteration is quantized.

To allow a quasi-simultaneous particle tracing, the time when the sound particle hits the patch has to be quantized, too. This is the next step: the temporal quantization. Therefore the timeline from $t = 0$ to $t = T_{max}$ is quantized in time intervals Δt, where T_{max} is the maximum time of interest. As a first approach (that is discussed in the later section on accuracy), these time intervals are made proportional to the patch length:

$$\Delta t \cdot c = l_P = \frac{c}{g_P}, \tag{3a}$$

where c is the speed of sound. The number of these time intervals is

$$\frac{T_{Max}}{\Delta t} = \frac{c \cdot T_{Max}}{l_P} = \frac{c \cdot T_{Max}}{c} \cdot g_P. \tag{3b}$$

The particle hit-times on the surface are moved to the middle of these time intervals.

The adjustments to the middle of the patch as well as to the middle of the time interval become relevant in the next iteration step.

Sound particles shall be unified if they have the same start patch, end patch and time interval number. To find such identical sound particles, a re-unification matrix (RUM) is introduced. The RUM is the core of the sound particle radiosity method as well as the main memory of the algorithm. The RUM reserves an entry for the energy of every possible sound particle. The size of this memory is big, as memory has to be reserved *for any start patch to any end patch at any time* (see Figure 9).

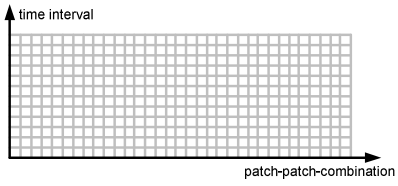

Figure 9. A re-unification matrix reserves an entry *for any start patch to any end patch at any time.*

The number of matrix elements K is the product of the number of possible start patches, the number of possible end patches (each being g_P according eqn. 2b) and the number of possible time intervals which is with eqn. 3b

$$K = \frac{c}{l_P} \cdot \frac{c}{l_P} \cdot \frac{T_{Max}}{\Delta t} = {g_P}^3 \cdot \frac{c \cdot T_{Max}}{c} \tag{4}$$

The number of matrix elements K, and with it the memory, increases with g_P, i.e. with smaller patch lengths, to the power of three - the big problem of the sound particle radiosity method. Each matrix element (ME) of the RUM only stores the energy of the sound particle it represents; start patch, end patch and time are encoded in the position of the ME in the RUM. When two sound particles are identical after quantization, the energies of both sound particles are placed in the same ME, where they are added – the moment of re-unification. The benefit is: they can be traced further on as one sound particle (even sound particles from different sources can be combined). By sorting every sound particle's energy into that matrix, an inefficient search for matching sound particles to combine is avoided.

The filling of the RUM shall be shown for an example in Figure 10.

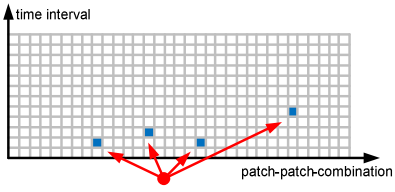

a) initialization (first filling of the RUM with energies from the original source)

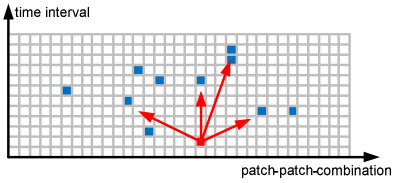

b) split-up of a sound particle into four new ones and transport of their energies to other matrix elements

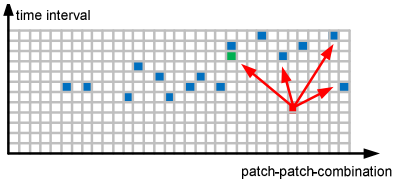

c) re-unification of two sound particles by adding a sound particle to an already set matrix element (green)

Figure 10. Illustration of the RUM for some iteration steps. On the $x - axis$, every possible patch-patch-combination has an entry, while for every time interval a row is reserved $(y - axis)$.

After initialising the RUM with four sound particles (Figure 10a), one of them is chosen for computation, and due to a split-up by scattering or diffraction, four new sound particles are placed back in the RUM (Figure 10b). The same in Figure 10c, but one of the sound particles hits an already occupied ME (green). In that element the energies are added such that a re-unification takes place. The optimum sequence of handling the sound particles (with the highest re-unification rate) can be summarized as "always the oldest sound particle first" (lowest row in the RUM). When using this sequence it is avoided, that a sound particle transports energy to a ME, from where another sound particle has already previously transported energy away. A second benefit when using the "oldest sound particle first" sequence, is that the maximum number of rows in the RUM needs not to be more than according the maximum free path length l_{Max}. This effect allows a reduction of the memory afford, because only MEs from the actual time t to $t + \frac{l_{Max}}{c}$ need to be addressed. So a cyclic buffer can be used, which can be interpreted as a 'va-

lidity tube' (or 'cloud of occupied ME') in the RUM as shown in Figure 11.

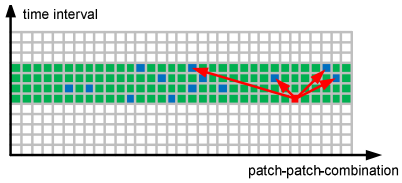

Figure 11. When using the "oldest particle first" sequence, only a time range corresponding to the maximum free path length is valid. This is shown as a green validity tube.

STATISTICAL ANALYSIS OF THE SOUND PARTICLE RADIOSITY ALGORITHM

Degree of occupation of the RUM and the re-unification rate

To evaluate the re-unification rate in the RUM, the number of occupied matrix elements, i.e. the degree of occupation of the RUM, shall be considered in a statistical way. To explain this approach, the following quantities are defined:

- K: number of matrix elements (ME) in the RUM
- N_B: number of occupied MEs (filled with sound energy). It can be understood as number of simultaneously existing sound particles. N_B is the decisive number that shall be expressed as a function of the number of iterations i or order o
- B: ratio of occupied MEs relative to the maximum number of MEs. $B = {N_B}/{K}$ (**`degree of occupation'** of the RUM)
- N: number of sound particles emitted from the source(s)
- S: additional number of sound particles generated recursively (see scattering section)
- i: counter of all computed iterations (reflections, scatterings or diffractions) since emission
- o: the classical reflection order, now including scattering and diffraction

exact definition of o: within one 'order' all sound particles (and MEs) of previous order $N_B(o-1)$ ('one layer' in Figure 4) have to be handled once. Hence, the additional number of iterations is

$$\Delta i(o) = N_B(o-1), \tag{5a}$$

or for the next order respectively

$$\Delta i(o+1) = N_B(o) \tag{5b}$$

Regarding eqn. 5a, the number of computed iterations i to reach order o can be calculated to:

$$i(o) = i(o-1) + \Delta i(o) = i(o-1) + N_B(o-1) \tag{6a}$$

Instead by this recursion formula, $i(o)$ may also be expressed as the number of all occupied ME ever having existed:

$$i(o) = \sum_{p=1}^{o} N_B\,(p-1) \qquad \text{with } N_B(0) = N \tag{6b}$$

To distinguish both parameters i and o Figure 4 can be consulted. While the reflection order o can be seen as the layer, the number of iterations i is the number of line segments below this layer (eqn. 6b).

Now, the number of occupied MEs N_B, the degree of occupation of the RUM and hence the re-unification rate shall be expressed as a function of i or o. They depend in a complicated way on different parameters, also strongly on the room shape. Nevertheless a statistical evaluation is tried in the following.

Case without re-unification

To demonstrate N_B, it shall be considered without re-unification, i.e. with an infinite number of MEs ($K \to \infty$). Without split-up ($S = 0$) is $N_B = N = const$. With a split-up of sound particles ($S > 0$) with each iteration, the energy of one ME is taken out of the RUM and is distributed over $S+1$ other MEs. So the balance (and recursion) formula for the number of occupied MEs in the RUM is

$$N_B(i+1) = N_B(i) - 1 + (S+1) = N_B(i) + S \tag{7}$$

With the initial state $N_B(0) = N$ the direct function $N_B(i)$ easily can be found:

$$N_B(i) = N + i \cdot S \tag{8}$$

So, the number of occupied MEs grows linearly with the number of iterations i.

More convenient, in the sense of what is in common use, is to express the growth of N_B as a function of the order o. To reach the next order $o+1$, according eqn. 5b, $\Delta i(o+1) = N_B(o)$ iterations to be computed. Also $N_B(o)$ MEs are occupied before. To find the necessary recursion formula, eqn. 8 can be consulted. Eqn. 8 presents the number of occupied MEs after i iterations, when at beginning N MEs are occupied. This statement is independent from previous processes. Hence, to compute the number of occupied MEs of order $o+1$, the scheme of eqn. 8 can be used replacing N by $N_B(o)$ and i by $\Delta i(o+1)$ additional iterations. This yields the recursion formula:

$$N_B(o+1) = N_B(o) + \Delta i(o+1) \cdot S = N_B(o) \cdot (1+S) \tag{9}$$

Solving again the recursion with $N_B(0) = N$ yields

$$N_B(o) = N \cdot (1+S)^o \tag{10}$$

So, the number of occupied MEs increases exponentially with o. The difference between the linear growth of N_B as a function of i (eqn. 8) and the exponential growth of N_B as a function of o (eqn. 10) can be explained by accepting that the number of necessary iterations i grows itself exponentially with the order o. The increasing number of sound particles is proportional to the computation time and, hence, makes the simulation inefficient and impossible for higher orders.

Case with re-unification

Now we consider that the total number of MEs K is finite (eqn. 4). Then, during the energy transfer iterations, there is a certain probability p_r to meet an already occupied ME. This is the re-unification probability. The rest probability, i.e. to meet an unoccupied ME, is $(1-p_r)$. The energy taken out of one ME is still distributed to $S+1$ other MEs with each iteration, but only $(S+1)\cdot(1-p_r)$ empty ME will become occupied in addition, thus, the 'growth- equation' 7 mutates to

$$N_B(i+1) = N_B(i) - 1 + (S+1)\cdot(1-p_r) \tag{11}$$

For statistics, we need a simple and reasonable assumption for p_r. The standard assumption of statistical room acoustics, i.e. of reverberation theory, is the 'diffuse sound field'. This means that

a) the sound energy is homogeneously distributed in space and

b) each direction is equal probable.

So, the occupation of all start patches as well as the striking of all target patches on the surface is equal probable. Hence, all MEs in the RUM are equally probably occupied (at least after many iterations).

With the assumption of equal distribution and the degree of occupation, the re-unification probability p_r is assumed to be constantly the number of occupied ME relative to their total number K

$$B = {}^{N_B}/_{K} = p_r \tag{12}$$

Inserting eqn. 12 into eqn. 11 yields a new recursion formula for the occupied MEs with re-unification

$$N_B(i+1) = N_B(i) - 1 + (S+1)\cdot\left(1 - \frac{N_B(i)}{K}\right), \tag{13}$$

where the initial value $N_B(0)$ is the number of originally emitted sound particles N. By some analysis, this recursive eqn. 13 can again be converted into an explicit function of i

$$N_B(i) = N\cdot q^i + \frac{S}{S+1}\cdot K\cdot\left(1-q^i\right) \tag{14a}$$

$$\text{with} \qquad q = 1 - \frac{S+1}{K} \tag{14b}$$

The number of occupied MEs of the RUM may be interpreted as the number of simultaneously existing sound particles. It is shown in Figure 12 for different split-up degrees S compared with the number of simultaneously existing sound particles of the SPSM, i.e. without re-unification.

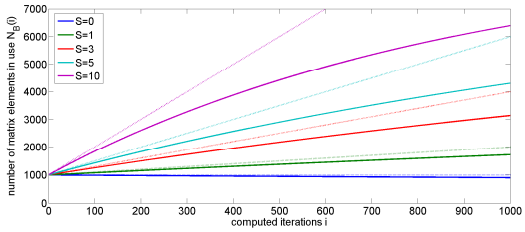

Figure 12. Comparison of simultaneously existing sound particles of the SPSM (doted lines) and the SPRADM (solid lines) for different split-up degrees S.

It can be seen, that for different split-up degrees S the increase of the number of parallel existing sound particles is different. The graphs for the numbers of sound particles without re-unification are straight lines (eqn. 8), while with re-unification the number of simultaneously existing sound particles is much lower (for $S = 0$ even decreasing) due to re-unification (eqn. 14). The difference is the benefit of re-unification.

More comprehensive would it be, again, to discuss the number of occupied MEs as a function of the order o. The respective recursion formula for $N_B(o)$ can be deduced from eqn.14a in a similar way as eqn. 9 has been deduced from eqn. 8: The role of a former number of occupied ME, N, plays $N_B(o)$, the number of necessary iterations i to reach $N_B(o+1)$ (the number of ME of order $o+1$) is $\Delta i(o+1) = N_B(o)$ (both assumption as before). Thus, from eqn. 14a follows

$$N_B(o+1) = N_B(o)\cdot q^{N_B(o)} + \frac{S}{S+1}\cdot K\cdot\left(1-q^{N_B(o)}\right) \tag{15a}$$

$$\text{with } q = 1 - \frac{S+1}{K} \tag{15b}$$

(During one generation of iterations of order o, all MEs have to be handled once. During this process, some MEs to compute might receive sound particle energies, which will - as not yet handled itself- be transferred further together with the energy having been before in this ME. So, during one generation, some sound particles might be reflected, scattered or diffracted more than once. Thus, with re-unification, the definition of 'order' becomes doubtful; the effective order might be higher than assumed.)

From this complex recursion formula the explicit function $N_B(o)$ can be computed only numerically. The result is here displayed just graphically (see Figure 13).

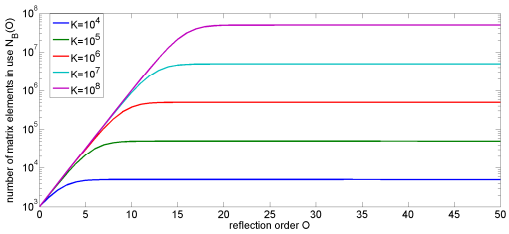

Figure 13. Comparison of simultaneously existing sound particles of the SPRADM for different sizes of the RUM K as a function of the reflection order o (note the logarithmic y axes)

It can be seen, that at low orders the number of occupied MEs, i.e. the number of simultaneously existing sound particles, per order growths exponentially (linear in a logarithmic scale, Figure 13) as expected without re-unification. After a critical order, the number of simultaneously existing sound particles converges to a constant value. Then, the number of iterations to be performed to manage one reflection order is constant, and so the computation times increase only linearly with the order o. The upper limit for simultaneously existing sound particles is hardly dependent on the split-up degrees for high split-up degrees and almost only dependent on the number of accessible RUM elements K. As can be directly derived from eqn. 14a,

$$N_B(o\to\infty) = N_B(i\to\infty) = \frac{S}{S+1}\cdot K \tag{16}$$

Eqn. 16 shows, that the degree of occupation $B = \frac{N_B}{K} = \frac{S}{S+1}$ tends to full occupation for high split-up degrees S. If only a small portion f of the room's surface is scattering or diffracting, such that $S = f\cdot s < 1$, then the degree of occupation is $< {}^1/_2$. Without split-up ($S = 0$) the degree of occupation convergates even to zero. In the statistical assumption that is plausible, because no split-up compensates the re-unification (even if probability to re-unify is low in that case).

The smaller the patches are, i.e. more patches for same scene, the lower is the re-unification rate p_r and the closer is q to 1 in eqn. 14b. Hence, a higher order is needed to suffer of re-unification. To achieve a high re-unification rate and a reduction of computation time, it must be the aim to minimize the size of the RUM.

Different assumptions than the equally distributed MEs in the RUM

The assumption of diffuse sound field, and with it the equally distributed MEs in the RUM, are only a first rough approximation. In reality, some patches in far corners are less probably occupied; others may be more probably occupied due to focussing effects. In later iterations, sound particles will again tend to concentrate there. So, with unequal distribution, the effective re-unification probability will be greater than N_B/K, as if the 'effective' number of reachable MEs K would be smaller. Therefore N_B will propably grow a bit slower than assumed in the following.

The convex sub-division of large scenes generates sub-scenes, where more sound particles exist simultaneously and thus the re-unification rate increases in such areas – at the cost of lower re-unification rates near areas with fewer sound particle density.

Although there are less probably hit MEs, the memory does still have to be reserved. No reduction of memory can be expected.

Measurement of computation times of the sound particle radiosity method and comparison to the sound particle simulation method

The aim is to analyse the computation time of the new SPRADM compared with the SPSM in the classical way, i.e. as a function of the order o. The computation time of the simulation is proportional to the number of computed iterations i, i.e. handlings of reflections, scatterings and diffractions.

The classic sound particle simulation method (i.e. without re-unification) as well as the sound particle radiosity method (i.e. with re-unification) have been implemented and simulations for a simple rectangular room and a split-up degree $S = 25$ were performed.

A problem for the statistical evaluation is: The maximum reflection order o, as a well known truncation criterion for the SPSM, can not be used directly for SPRADM, because not exact order is defined due to re-unification. On the other hand, an energetic truction criterion is in use (This is practically necessary to avoid almost endless oscillations of sound particles between close surfaces in pathological cases). Sound particles are aborted after their energy decreases by a factor of E_{min}.

So, a new feature has to be introduced: the room absorption. A mean absorption degree for all surfaces is named α. On average, with each iteration, every sound particle loses energy according the factor $(1-\alpha)$ due to absorption and according $1/S+1$ due to split-up. In these simulations, α was set to 0.5 at all surfaces such that the factor $\left(\frac{1-\alpha}{S+1}\right)$ was about 0.02.

While every sound particle energy decreases with each order (i.e. $E_{min} = 0.02^o$), a fictive mean order o to abort is

$$o_{Max} = \frac{\log(E_{min})}{\log(0.02)} \tag{17}$$

which replaces the former definition of the reflection order o.

The result for one of these simulations is shown in Figure 14.

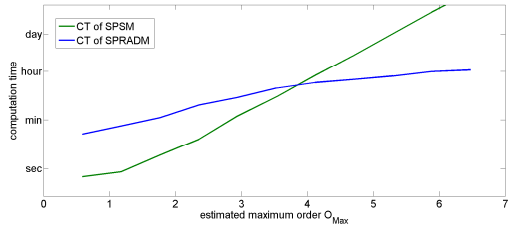

Figure 14. Comparison of computation time of SPSM (without re-unification) and the SPRADM (with re-unification) as a function of order o for a simple rectangular room and a split-up degrees of $S = 25$ with logarithmic y - scale

While the computation time grows exponentially for the SPSM, which is linear in logarithmic scale, the computation time of the SPRADM has a decreasing slope in logarithmic scale. That slope converges to a constant value in linear scale (not displayed here), i.e. the computation time per order becomes constant. That follows from the fact that with the SPRADM an almost constant number of sound particles are interchanged between the MEs of the almost fully occupied RUM (see Figure 13). This is a drastic increase of efficiency.

On the other side, a quite high computation time for lower orders can be observed. This additional computation time can be described as an overhead due to searching (taking out and placing back sound particles energies) in the RUM. This storing time lets the overall computation time increase as long as there are only few re-unifications. The measured computation times for memory usage and actual sound particle tracing are displayed separated in Figure 15.

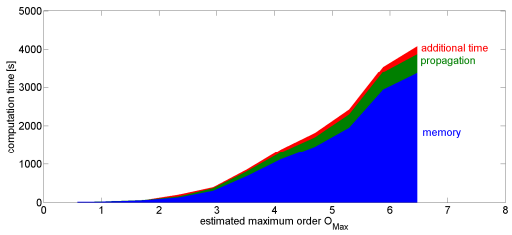

Figure 15. Separation of computation time of the SPRADM with re-unification in memory, sound particle tracing and additional time due to different processes

Further investigations showed that the time of memory usage is about proportional to the computation of particle tracing. The memory computation time has been here about 6 times as long as the computation time for particle tracing. Therefore, for lower orders, the SPRADM is even more inefficient than the SPSM; it is only effective for higher orders.

Accuracy compared to the SPSM

Of course, the quantization of the room's circumference (in 3D: surface) lowers the accuracy of the simulation. To quantify this accuracy loss, echograms for the SPSM and the SPRADM are compared. Again the rectangular shaped room has been chosen and a high number of $N = 1000000$ sound particles have been emitted to allow the SPSM to be used as a reference [11]. First evaluations were performed without split-up, because otherwise the computation times of the SPSM would be too large. The mean wall absorption was again set to $\alpha = 0.5$. Different echograms computed by the SPSM and the SPRADM for typical patch sizes are shown in Figure 16. The patch length is expressed as a portion of the

mean free path length (MFPL) by the factor f_P according eqn. 2a. The receiver (detector) diameter has been stantly $1m$.

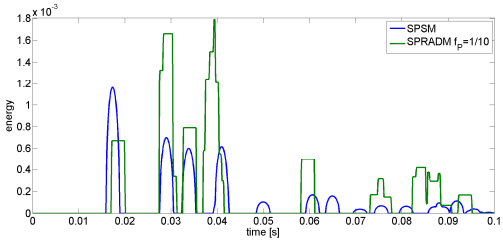

a) specific patch size $f_P = {}^1/_{10}$

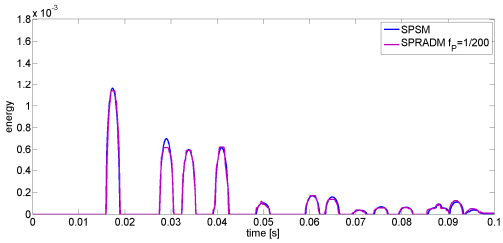

b) specific patch size $f_P = {}^1/_{200}$

Figure 16. Comparison of echograms computed with SPRADM and different patch sizes with the unquantized SPSM for a specified listener position (diameter $1m$) in a rectangular room.

The echogram of the SPRADM with $f_P = {}^1/_{10}$, i.e. 10 patches per MFPL, is totally different from the reference curve of the SPSM. But with smaller patches the echograms become more similar until the SPRADM with $f_P = {}^1/_{200}$ matches quite well the reference curve.

In our investigation three kinds of errors were determined:

- error in total energy
- error in time interval
- error in reverberation time

The error in total energy is computed as the relative difference of the energy summations of the SPRADM echogram relative to the SPSM echogram.

To compute an energetic error in time intervals, the absolute difference of energy in all small time intervals (of $\Delta t = 10ms$, reasonable to compute room acoustic parameters) is computed, summed up and normalised to the total energy of the SPSM echogram.

The reverberation time T for SPSM as well as for SPRADM is computed with backwards integration of the echogram and linear regression. The displayed error is the relative difference in T between both simulation methods.

All three errors are shown in Figure 17 based on the average over four echograms as presented in Figure 16.

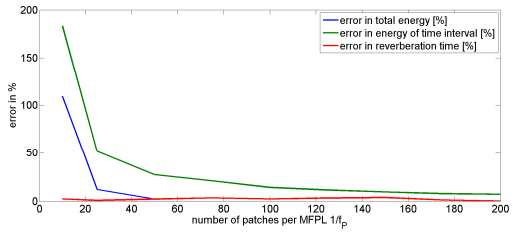

Figure 17. Relative errors of the SPRADM relative to the SPSM in total energy, energy in time intervals and in reverberation time as a function of the number of patches per MFPL without split-up

First of all it can be seen, that the error in total energy as well as the error in the time intervals decrease with smaller patches, i.e. more patches per MFPL. One can see, that very small patches in the size of ${}^1/_{200}$ of the MFPL still cause an error in the time intervals of about 7%. The error of total energy decreases faster, as it is about 2% starting with a patch length of ${}^1/_{50}$ of the MFPL. The error of the reverberation time is very low and almost not dependent on the patch size. The reason is that the reverberation time is only a value for the mean energy loss in the room. Even when there are large errors in particle directions and intersections points, the mean energy loss of each sound particle matches quite well the energy loss of the SPSM. Even if now totally different sound particles are detected, the energy losses, and thus the reverberation times, are hardly modified.

Further investigation showed, that all three errors are hardly dependent on the number of emitted sound particles, as long there are about 50 sound particles immitted at every patch.

In the next step a split-up of sound particles is introduced and the same errors are computed as above. The errors for different split-up degrees S are depicted in Figure 18.

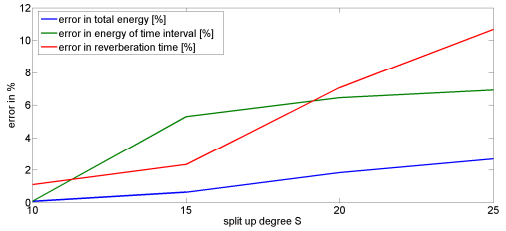

Figure 18. Relative errors of the SPRADM relative to the SPSM in total energy, energy in time intervals and in reverberation time for 100 patches per MFPL and different split-up degrees

All three errors increase with the split-up degree. That strange behaviour is not easy to understand, an influence of the split-up degree is not plausible (or if, then vice versa). To analyse this effect, an echogram of the SPSM and the SPRADM for a split-up degree of $S = 25$ is shown in Figure 19.

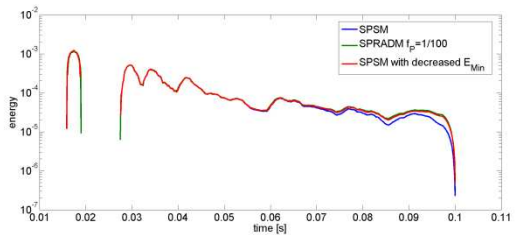

Figure 19. Comparison of an echogram of SPRADM, SPSM and SPSM with reduced energy criterion for a specified listener position in a rectangular room

The echograms show, that the error is generated in the late part of the echogram, where the SPSM has a lower energy than the SPRADM. Both simulations were aborted at the same minimum energy in the MEs. A diminishing of the minimum energy lets the level in the later part of the echogram increase as more sound particles 'survive'. The same effect occurs when the energies of several sound particles of each less than the minimum energy are added ('re-unified') in a ME. Then the minimum energy is exceeded by their sum and a computation of further iterations becomes possible. The result is the obeyed increasing accuracy of the SPRADM for higher split-up degrees. So, the apparent 'error' of the SPRADM is actually an error of the SPSM in the late echogram. That effect indicates by the way that any minimum energy criterion actually should be avoided, because the low energies of many sound particles may cumulate.

Also other quantised time intervals Δt proportional to the patch length were tested. No great difference in the accuracies showed up, as long the time intervals times c were not larger than the patch length. Even with shorter time intervals, no increase of accuracy could be found, because the error is superposed by the error of patch quantization. So $\Delta t \cdot c = l_P$ (eqn. 3a) seems to be a good compromise.

Optimum quantization of the SPRADM

Finally the error depending on the patch length shall be estimated quantitatively. Therefore the main error criterion of the SPSM is consulted. With the SPSM, the relative error of the immitted intensity D depends on the number N_D of sound particles having crossed the detector (receiver). Assuming the law of a normal distribution, this reads $D = {N_D}^{-1/2}$. With the SPRADM the distance of sound particles flying in parallel (freely varying with the SPSM) is always in the magnitude of the patch size. So, to keep the number of sound particles intersecting a receiver reasonable, the first approach is to couple the receiver size with the patch size. A reasonable assumption is to make them four times larger than the patches. So, now simulations with a flexible receiver diameter of four times the patch length were performed; the errors are shown in Figure 20.

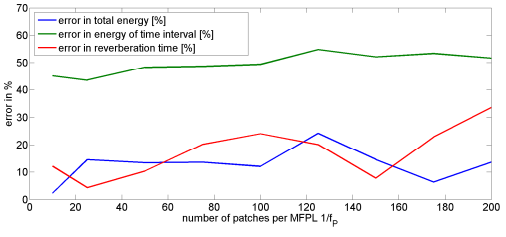

Figure 20. Relative errors of the SPRADM relative to the SPSM for different patch sizes with variable receiver size of four times the patch length

The errors are now only hardly dependent on the patch length, although the patch length variates from $1/200$ to $1/10$ of the MFPL. The same investigation for a variable receiver size of forty times the patch length showed also quite constant errors only changing with a maximum factor of 2. These results lead to the final investigation in which the patch size is held constant, but the receiver diameter is varied. The results (see Figure 21) show the quite expected $D = {N_D}^{-1/2}$ law.

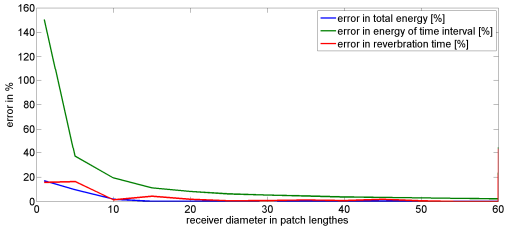

Figure 21. Relative errors of the SPRADM relative to the SPSM in total energy, energy in time intervals and in reverberation time for constant patch size, but different receiver sizes.

A good compromise of accuracy seems to be a receiver size of 10…20 times the patch length. Then the relative errors of the total energy and of the reverberation time are below 5%, the error in energy of time interval is about 10%.

In real requirements the receiver size is not very flexible, as it leads to a decrease in the spatial resolution of sound simulation. As a result the optimization condition has to be inverted:

When a certain spatial resolution is wanted (which might be related to an average size of 'small' surfaces), the receiver size is fixed to that resolution. Based on the receiver size, the patch size of the SPRADM can be determined as about 10% of the receiver diameter (or smaller for higher accuracy).

Finally other room geometries were investigated. Due to the large memory afford, only small and simple scenes could be computed. The results were quite the same as for the rectangular room, even for non convex rooms (Except for cases with very close walls with a small angle between causing particle oscillations between the walls distorting the statistics).

CONCLUSION AND OUTLOOK

We presented an energetic combined sound particle radiosity method as an algorithm for the computation of sound propagation including reflections and scatterings of arbitrary order. By quantization of the surfaces (as with the radiosity method) and the angles (as with the SPSM) a re-unification is enabled.

Sound paths are not computed one after another but almost in parallel utilizing a re-unification matrix (RUM). A statistical analysis showed that the RUM is nearly full for higher orders with split-up. Measurements showed a reduction of computation time from exponential to linear growth with split-up of sound particles. Without split-up, almost no re-unification takes place and the SPRADM becomes ineffective.

Two concurring requirements determine the SPRADM. On the one hand, more and smaller patches let the accuracy increase. On the other hand, fewer and larger patches increase the re-unification rate and thus the efficiency. The optimum patch size has to be determined for any application.

The main problem of the algorithm is the huge memory effort, such that complex geometries cannot be computed with high accuracies. For low scattering orders the search overhead in the memory pushes up the computation time.

Further investigations will have to aim at a more efficient search in the RUM combined with a reduction of the necessary memory space. Current research is devoted to reduce the size of the RUM by skipping the 'same time' criterion for reunification. To compensate this, no single sound particles, but groups of 'younger and older' sound particles on the same path (respectively partial echograms), are traced and stored in the new RUM.

Before the memory problem is solved for the sound particles radiosity method, an implementation of quantised pyramidal beam tracing is not practicable, because its memory need is even greater.

REFERENCES

1 T. J. R. Hughes, *The Finite Element Method: Linear Static and Dynamic finite Element* Analysis (Dover Publications, 2000)

2 O. Von Estorff, *Boundary Elements in Acoustics: Advances and Applications* (WIT Press, Vol. 9, 2000)

3 J. Borish, "Extension of the image model to arbitrary polyhedral", *J. Acoust. Soc. Am.* **75**, (1984)

4 M. Vorländer, "Simulation of the transient and steady-state sound propagation in rooms using a new combined ray-tracing image source algorithm", *J. Acoust. Soc. Am.* **86**, (1989)

5 A. Farina, "a New Pyramid Tracer for Medium and Large Scale Acoustic Problems", *Proceedings of Euronoise (1995, Senlis, France*)

6 R. N. Miles, "Sound field in a rectangular enclosure with diffusely reflecting boundaries", *J. Sound and Virbration*. **92**, (1984)

7 H. Kuttruff, *Room Acoustics* (Taylor & Friends, 5th Edition, 2009)

8 U. P. Svensson and R.I. Fred, "An analytic secondary source model of edge diffraction impulse responses", *J. Acoust. Soc. Am*. **106**, (1999)

9 U. M. Stephenson, "An improved energetic approach to diffraction based on the uncertainty principle", *Proceedings of ICA 2007* (Madrid)

10 U. M. Stephenson, "Quantized Pyramidal BeamTracing or a Sound-Particle-Radiosity-Algorithm?", *Proceedings of research symposium* (Inst. of Acoustics, Salford, 2003)

11 A. Pohl and U. M. Stephenson, "From ray to beam tracing and diffraction – an analytical prognosis formula for the trade-off between accuracy and computation time", *Proceedings of DAGA 2010* (Berlin)

12 A. Pohl and U. M. Stephenson, "Efficient simulation of sound propagation including multiple diffractions in urban geometries by convex sub-division", *Proceedings of Internoise 2010* (Lisbon)